INTERNATIONAL CONFERENCE ON ADVANCES IN TECHNOLOGY AND COMPUTING (ICATC-2021)
Faculty of Computing and Technology (FCT), University of Kelaniya, Sri Lanka
18th December 2021

Index No: ES-12-20

Field Testing of Highway Bridges Enhanced by Assumptions of Composite Action

Renxiang Lu (1st Author)
Department of Civil and Architectural Engineering
University of Wyoming
Laramie, Wyoming, USA
rlu@uwyo.edu

Johnn Judd (2nd Author)
Department of Civil and Construction Engineering
Brigham Young University
Provo, Utah, USA
johnn@byu.edu

***Abstract* — A load rating procedure that involves field testing and composite action considerations for girders affected by external effects is presented in this paper. In the proposed procedure, the critical vehicle sequence for the bridge is determined and the actual response of the bridge is measured using a series of runs by driving a vehicle of calibrated weight. To replace the data readings affected by external effects, the position of the neutral axis corresponding to a fully composite action is assumed. After applying this correction, the actual load rating is discretized and compared with the analytical load rating so that different contributions to the loading capacity are quantified. A three-span non-composite steel girder highway bridge was used to illustrate the procedure. Results indicate that although the unintended composite action was the dominant contribution, the contribution was unreliable for loads beyond the linear elastic regime. It was observed that corrections made based on composite action assumptions improve the understanding of the case study because the contributions due to additional stiffness lateral and longitudinal distribution would have been unrealistic otherwise.**

Keywords* — *Field testing, composite action, load rating

I. INTRODUCTION

Highway bridges are essential to allow people to commute over physical or man-made obstacles, but the loading capacity of highway bridges can diminish over time for a variety of reasons. Fatigue, caused by quotidian traffic, damages caused by accidents, as well as impacts due to adverse environments, are common causes for a reduction in bridge load capacity [1]. Fortuitously, there can be additional inherent "reserve" load capacity in bridges which is not accounted for in the routine design. For example, the additional stiffness contributed by curbs, barriers and railings can change the load path and can increase load capacity [2]. Similarly, the actual load distribution within the bridge span, between the piers and abutments, can be significantly different from the theoretical distribution [3]. Partial restraint of the supports due to accumulation of debris can alter the distribution of load [4]. Composite action between the bridge girders and the bridge deck can also occur, even if the bridge was designed to act non-compositely [5]. Although partial restraint of the supports and unintended composite action can be unreliable contributions to capacity, an understanding of these effects is necessary to determine the overall load-carrying capacity of the highway bridge. In contrast to conventional design practice, i.e., application of theoretical equations given in the codes and specifications, non-destructive field testing is an effective way to evaluate unintended composite action and to determine the reserve load capacity.

II. OBJECTIVES

This paper presents a procedure to obtain the actual loading capacity of a typical highway bridge based on experimental non-destructive field testing coupled with a determination of composite action. In brief, the procedure consists of determining the critical vehicle sequence for the bridge, obtaining the actual internal response of the bridge under vehicular loads, and comparing the measured response with the analytical response to systematically identify reliable and unreliable contributors to the loading capacity. The procedure is demonstrated using a three-span non-composite steel girder highway bridge with a concrete deck.

III. METHODOLOGY

In this section, the procedure of a non-destructive bridge field testing coupled with assumptions of composite action is described and applied to a case-study bridge located in Laramie, Wyoming (United States). After identifying the relevant properties of the bridge for the analysis, girders were instrumented with strain gauges at the maximum positive and negative moment positions. A vehicle with calibrated weight is driven across the entire bridge at distinct transverse locations in to order to capture the response for every girder. The responses are collected in form of strain histories in which the corresponding time to the peak strain is identified. The strains associated with this time are used to compute strain profiles which are therefore employed for the calculation of internal moments and axial forces, separating the non-composite and composite action components. For the collected data that was affected by external effects unanticipated in the field testing, corrections on the load rating calculation are made based on fully composite action assumptions. The fully composite neutral axis is used to replace the strain readings that were impaired. With that, the actual load rating is calculated, and its corresponding live load effects are discretized. By comparing it with the existing load rating, the contributions due to longitudinal and lateral

distributions, additional stiffness in the system, deck flexure, and unintended composite action are disaggregated.

A. Laramie Bridge

The methodology described above was illustrated using the westbound highway bridge on Interstate 80 over the Laramie River in Laramie, Wyoming. The bridge is non skewed and has three spans (Fig. 1). The outer spans are 18.3 m (60 ft) each, and the inner span is 22.9 m (75 ft). The original bridge was built in the 1960s with four nominally identical I-shape steel girders that were designed to be non-composite (Girders 1 through 4 in Fig. 2). The bridge was later widened by adding a fifth I-shape steel girder (Girder 5 in Fig. 2). This girder was still designed to act non-compositely, but a metal sheet was poured below the deck which connects it with Girder 4 to confer a higher bonding. All girders are bisymmetric, and the dimensions are identified in Table 1. The clear roadway width is 12.2 m (40 ft), and the deck is 191 mm (7.5 in.) thick in addition to an overlay of 25.4 mm (1 in.) throughout the whole bridge. The girders are supported by expansion bearings, except at the outer pier on the west side which is supported by a fixed bearing. Typical X-bracing cross-frames are present at the piers and steel diaphragms are present on the abutments. Also, X-bracing cross-frames are spaced 6.10 m (20 ft) on the outer spans and 7.62 m (25 ft) on the inner span.

The critical moment positions for the Laramie Bridge occur at the western outer span at the 0.4 times of the outer span measured from the abutment for the positive moment, and at the pier for the negative moment. For comparison purposes, the actual responses of the same longitudinal positions for positive and negative moments were determined. Thus, all girders at the corresponding positions were instrumented with ST350 strain gauges [6]. At the positive moment, each girder received three strain gauges: at the center of the bottom flange, on the web at a position 254 mm (10 in.) and 508 mm (20 in.) above the bottom of the bottom flange. At the negative moment, each girder received two strain gauges: at the center of the bottom flange, and on the web at a position 508 mm (20 in.) above the bottom of the bottom flange. It is recognized that this setup only allows the calculation of the live load effects.

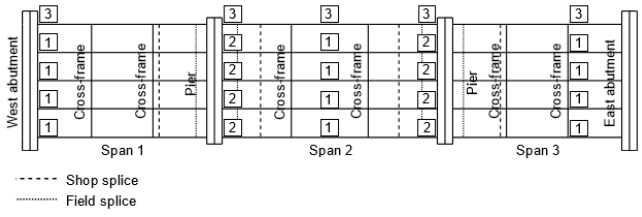

Fig. 1. Plan view of the Laramie bridge.

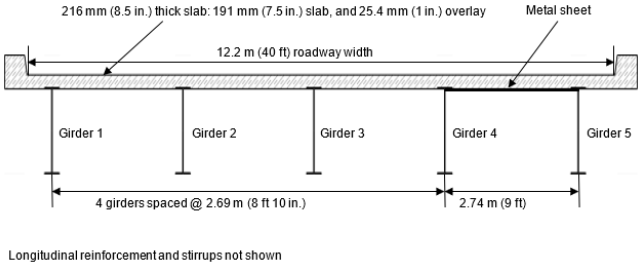

Fig. 2. Cross-sectional view of Laramie bridge (direction of traffic).

Table 1. Nominal section girder dimensions, mm (in.) for locations identified in Fig. 1.

Location	Flange		Web	
	Width	Thickness	Width	Thickness
1	305 (12)	19.1 (0.75)	1300 (51)	9.53 (0.38)
2	305 (12)	25.4 (1.00)	1300 (51)	9.53 (0.38)
3	305 (12)	19.1 (0.75)	1300 (51)	11.1 (0.44)

B. Instrumentation and Field Testing

In the field test, a vehicle with calibrated weight was driven at crawl speed over the bridge in successive runs that traverse the width of the roadway according to the requirements given in *The Manual for Bridge Evaluation* [7]. A total of fifteen runs were conducted to obtain the maximum responses for every girder. The runs were conducted from right to left, relative to the direction of travel. In the first run, the center of the right front wheel was positioned 0.91 m (3 ft) from the right curb. The position of each successive run was 0.61 m (2 ft) offset to the left of the previous run (Fig. 3). As a non-destructive field test, the vehicular load was selected so that responses generated on the bridge are within the linear elastic regime. To simulate side-by-side vehicle loadings, responses obtained in individual runs are superimposed.

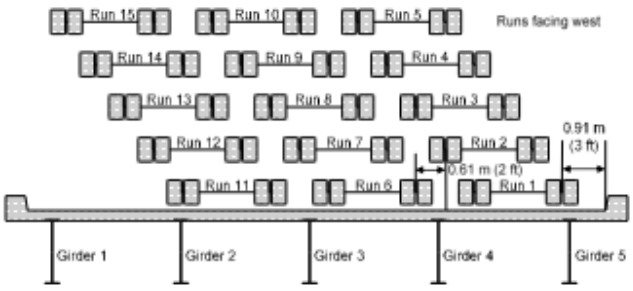

Fig. 3. Transverse position of successive runs of the field testing.

During the field test, a strain history (i.e., a graph that illustrates the strain variation over time due to the vehicle) was collected for every girder and run. For each run, the girder with the peak strain and the corresponding time of occurrence were selected. This girder was identified as the critical girder for the run. The time that the peak strain occurred was also applied to the other strain gauge of the critical girder so that a linear strain profile was computed

(Fig. 4). The same selected time was also applied to all the non-critical girders to obtain their respective strain profiles. For the negative moment, the peak strain when the vehicle was at the outer span was selected instead. Although a larger strain occurs when the vehicle is on the inner span, this time is not used because it does not allow the statical moment to be calculated, which is used later to determine the actual live load. At the positive moment, the strain profiles were obtained based on the best fit least square regression line since three strain gauges were mounted on each girder, while at the negative moment, the strain profiles were obtained by linearly connecting the strain readings on the two strain gauges mounted on each girder.

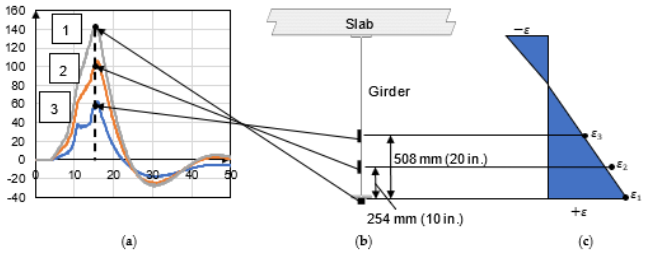

Fig. 4. Computation of a strain profile at the positive moment location: (**a**) strain history and maximum strains; (**b**) bridge cross-section; (**c**) strain profile.

C. Data Reduction

Live load internal stresses were calculated based on the measured strain profile and the material and geometric properties of the girder and the deck. The calculated total live load internal stress profile (Fig. 5(a)) was decomposed into a live load axial component (Fig. 5(b)) and a live load flexural component (Fig. 5(c)). The girder live load axial stress, σ_{cg} is equal to the total stress at the center of gravity of the girder. The maximum girder live load flexural stress is equal to the live load total stress at the extreme fiber of the bottom flange, σ_0 minus σ_{cg}. The live load axial force in the girder, N is equal to the product of σ_{cg} and cross-sectional area of the girder. The live load axial force in the deck was assumed to be equal to N to maintain the equilibrium of the system. The live moment of the girder, M_{girder} was obtained as the product of the girder live load flexural stress and the girder section modulus. The live load moment in the deck, M_{deck} is the product of M_{girder} and the ratio of the deck and girder flexural stiffnesses. The live load moment due to interaction between the girder and the deck was calculated as the product of N and the distance from the girder to deck centers of gravity, a. The total live load moment, M_{total} for the girder is the sum of the live load internal moments.

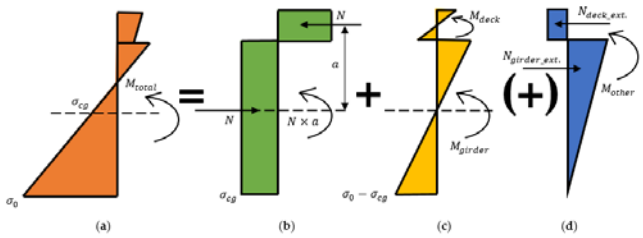

Fig. 5. Decomposition of a stress profile due to live load: (**a**) total stress; (**b**) axial stress; (**c**) flexural stress; (**d**) stress due to external effects.

The procedure of obtaining M_{total} was modified as some of the collected data seemed to be affected by external effects. It was observed that the neutral axis of Girder 1 through 4 was below the theoretical neutral axis even for runs that are transversely close to the respective girders. As an example shown in Fig. 6(a) and Fig. 6(b), which shows the stress profiles of Girder 2 and Girder 3 (most stressed girders according to Fig. 3 for Run 9), the neutral axes fall below the strain gauge mounted on the web at a position 508 mm (20 in.) (as a bisymmetric girder, the theoretically estimated non-composite neutral axis for Girders 1 to 4 at the positive moment is at the half-center line, a position 667 mm [26.3 in.] above the bottom of the bottom flange). This is contrary to the expectations since, even within the linear elastic regime, some composition action is expected [5]. The accidental placement of strain gauges at the area of influence of additional stiffeners present on the bridge is the most likely cause for these discrepancies (Fig. 7). It is likely that the out-of-plane restraints, as well as residual stresses accumulated between the stiffener and girder web may have impacted the readings on the strain gauges mounted on the girders' web [8], although strain gauges mounted on the bottom flanges were possibly affected in a lesser degree. This speculation is confirmed by the fact that the neutral axis on Girder 5 at the positive moment and on any girder at the negative moment were not affected, as no stiffeners are present on those positions.

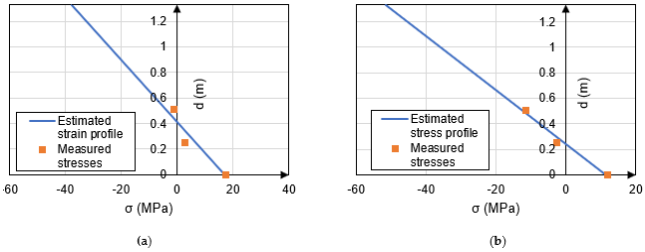

Fig. 6. Stress profiles affected by the transverse stiffeners for Run 9. (**a**) Girder 2. (**b**) Girder 3.

The inconsistencies showed above can be corrected by modifying the live load internal stress decomposition shown in Fig. 5(a), Fig. 5(b), and Fig. 5(c) by adding a new component as shown in Fig. 5(d). In this case, although the measured live load stress profile is unchanged, the live load axial component and the live load flexural component are obtained based on the measured stress at the bottom of the bottom flange and the assumption of a theoretically estimated

composite action to define the neutral axis position (considering, *a priori*, that the live load stress profile was affected by external effects). Under this condition, and assuming that the bottom strain gauge was not affected by the stiffener, σ_{cg}, the live load maximum girder flexural stress (σ_0 minus σ_{cg}), N, M_{girder}, and M_{deck} are calculated the same way as previously. Despite not being necessary for the computation of the internal moments for this study, a stress profile caused by the external effect is developed resulting from the balance with the assumed condition and measured stress profile. The geometry of the stress profile caused by the external effect is consistent with the hypothesis as the strain gauges on the web are expected to read additional stresses not accounted by the live load flexural nor axial components. Thus, a resultant force, $N_{girder\_ext.}$ and a resultant moment, M_{other} on the girder are shown. Since composite action is expected, a resultant force on the deck, $N_{deck\_ext.}$ may also exist to equilibrate the system.

In this approach, it was assumed that the readings for the strain gauge installed at the bottom of the bottom flange at Girder 1 through 4 were not affected by the transverse stiffeners. The readings of the strain gauges on the web were substituted by a theoretical neutral axis assuming a fully composite action behavior. Although the assumption is not conservative, it best describes the behavior of non-composite girders when subjected to loads within the linear elastic regime, as the bonding and friction between girder and deck are still not overcome [4]. It is recognized that the assumption does not cover the possibility of the girders having a partial composite behavior nor the actual behavior of the girders falling beyond the theorical limits. The theoretical fully composite neutral axis is located at the center of gravity of the combined system (girder plus deck). This is calculated based on principles of mechanics of materials, and the effective tributary width of the deck is estimated and converted into an equivalent width of steel, based on the modular ratio of steel to concrete. The fully composite neutral axis is equal to 1.19 m (46.8 in.) for Girder 1 and equal to 1.21 m (47.8 in.) for Girders 2, 3 and 4, measuring form the bottom of the bottom flange.

Fig. 7. Placement of strain gauges near transverse stiffeners.

D. Limit States Considerations

According to AASHTO, the loading capacity of highway bridges are obtained through calculation of the rating factor, *RF*, for each individual girder, with the lowest individual girder rating factor controlling the load rating of the bridge [9]. Among the different limits used to load rate bridges, the strength inventory *RF* is generally the most critical, and thus adopted in this research. As part of a research sponsored by the WYDOT (Wyoming Department of Transportation), since the bridge was originally designed and evaluated using the Load Factor Design (LFD) method and Load Factor Rating (LFR) limit states, respectively, the *RF* in this paper is also determined using the LFD method. Thus, all the analytical values are based on *Standard specifications for highway bridges* [10].

RF is defined as the ratio between the reserve capacity for live load and the limit state design live load and, in the LFD method, it is expressed in terms of the number of HS20 standardized design truck loads,

$$RF = (R_n\text{-}1.3D)/(2.17LL[1+I]) \quad (1)$$

where R_n is the capacity of the member, D is the dead load effect on the member, LL is the live load effect of the member, and I is the dynamic impact factor. If *RF* is greater than 1.0, the bridge is deemed adequate for the design load, and if *RF* is less than 1.0, the bridge is deemed inadequate. It was obtained by WYDOT that the analytical load rating at the critical positive and negative moment positions are 0.92 and 1.05, respectively.

IV. RESULTS AND DISCUSSION

In this section, the data reduction for the actual load rating is presented. Additionally, the disaggregated ratio of load ratings corrected based on fully composite action assumptions is also discussed.

A. Actual Load Rating

In this study, no inspections were conducted *in-situ* to determine the actual dead load effects of the bridge. As a result, it was assumed that the actual R_n and D are equal to the values obtained analytically. In addition, since no dynamic tests were conducted, the actual I was also assumed to be equal to the analytical.

The actual live load accounting for dynamic impact, $LL(1+I_E)$, is calculated as follows:

$$LL(1+I_E) = (M_{HS20}/M_{TRK\_OS})M_{girder} \\ (M_{TRK}/M_{TRK\_OS})m_E(1+I_E) \quad (2)$$

where M_{HS20} is the maximum analytical moment due to the HS20 design truck at the location of interest, M_{TRK} is the analytical maximum moment (positive or negative) due to the vehicle used in the field test, M_{TRK_OS} is the analytical maximum moment due to the vehicle used in the field test when the vehicle is at the outer span, m_E is the actual live load multi-presence factor, and I_E is the actual impact factor. The values of M_{TRK} and M_{TRK_OS} are theoretical values that were obtained using a line-girder analysis in which the vehicle used in the field was modeled as three concentrated loads and

placed at the critical moment positions (the same model that WYDOT used to obtain the analytical load rating). It was determined that M_{TRK} and M_{TRK_OS} are the same (since both occur at the outer span) and equal to 693 kN-m (511 k-ft) for the positive moment. For the negative moment, M_{TRK} (which occurs at the inner span) is equal to -455 kN-m (-335 k-ft), and M_{TRK_OS} is equal to -381 kN-m (-281 k-ft). As defined in the *Standard Specifications for Highway Bridges*, m_E accounts for the improbability of coincident maximum loading and is equal to 1.0 for single and 2-vehicle loadings, and equal to 0.9 for 3-vehicle loadings.

Based on the transverse positions of successive runs of the field testing shown in Fig. 3, a total of ten 2 side-by-side vehicle loadings and five 3 side-by-side vehicle loadings were considered. According to the experimental data, the two side-by-side vehicle loadings involving Runs 1 and 6 superimposed controlled (i.e., yielded the greatest $LL(1+I_E)$) at the positive moment, and the three side-by-side vehicle loadings involving Runs 3, 8 and 13 superimposed controlled at the negative moment. The controlling girder at the positive moment is Girder 5, and the controlling girder at the negative moment is Girder 3. The values of each variable to determine the load rating at the critical positive and negative moment positions are shown in Table 2. Thus, it was determined that $LL(1+I_E)$ is equal to 469 kN-m (346 k-ft) and -546 kN-m (-403 k-ft) at the positive and negative moment positions, respectively. As a result, the actual load rating at the critical positive and negative moment positions are equal to 1.75 and 1.53, respectively. The actual load ratings show that the bridge is deemed adequate at both critical moment positions.

Table 2. Values of variables for the calculation of the actual load ratings using Eq. (1) and Eq. (2).

Variables	Positive Moment	Negative Moment
R_n, kN-m (k-ft)	2300 (1700)	-2870 (-2110)
D, kN-m (k-ft)	406 (299)	-807 (-595)
M_{HS20}, kN-m (k-ft)	871 (642)	-784 (-578)
M_{TRK}, kN-m (k-ft)	693 (511)	-455 (-335)
M_{TRK_OS}, kN-m (k-ft)	693 (511)	-381 (-281)
M_{girder}, kN-m (k-ft)	294 (217)	-197 (-145)
m_E	1.0	0.90
I_E	0.27	0.26

B. Disaggregated Load Rating Comparison

The experimental load rating (RF_E) relative to the analytical load rating (RF_A) is defined as follows:

$$RF_E/RF_A = (M_{TRK\_OS}/M_{TRK})((\sum STAT_A/\sum STAT_E)$$
$$((DF_A \times m_A)/(DF_E \times m_E))(M_{LE}/M_{total})$$
$$(M_{total}/(M_{girder}+N\times a))(M_{girder}+N\times a)/M_{girder}) \quad (3)$$

where $\sum STAT_A$ and $\sum STAT_E$ are the analytical and actual statical moment, respectively, DF_A and DF_E are the analytical and actual live load distribution factor, respectively, m_A is the analytical live load multi-presence factor, and M_{LE} is the elastic longitudinal adjustment moment. The values of these variables at the critical positive and negative moment positions are shown in Table 3. Details for the calculation of each variable were shown in previous studies [3, 4].

Table 3. Values of the variables for the actual and analytical load rating comparison using Eq. (3).

Variables	Positive Moment	Negative Moment
$\sum STAT_A$, kN-m (k-ft)	1670 (1230)	2470 (1820)
DF_A	0.81	0.81
m_A	1.0	1.0
$\sum STAT_E$, kN-m (k-ft)	1320 (974)	2350 (1730)
DF_E	0.81	0.91
M_{LE}, kN-m (k-ft)	443 (327)	-331 (-244)
M_{total}, kN-m (k-ft)	454 (335)	-315 (-232)
$N\times a$, kN-m (k-ft)	150 (111)	-112 (-82.4)

Eq. (3) also shows the comparison of different contributions between the actual and analytical load ratings. The term (M_{TRK_OS}/M_{TRK}) is the contribution of the critical span adjustment, $(\sum STAT_A/\sum STAT_E)$ is the contribution of the additional stiffness in the system, $((DF_A\times m_A)/(DF_E\times m_E))$ is the contribution of the differences in lateral distribution, (M_{LE}/M_{total}) is the contribution of the differences in longitudinal distribution, $(M_{total}/(M_{girder}+N\times a))$ is the contribution of deck flexure, and $((M_{girder}+N\times a)/M_{girder})$ is the contribution of the unintended composite action. The disaggregation of the actual load rating is carried out based on principles of mechanics of materials, linear responses of the bridge, and equilibrium [3]. Note that in this case study, the same value is obtained by taking the inverse ratio of live load effects because R_n and D were kept constant. The values for each contribution are shown in Table 4.

Table 4. Values of the contributions for the actual and analytical load rating comparison using Eq. (3).

Contributions	Positive Moment	Negative Moment
Critical span adjustment	--	0.839
Additional stiffness	1.266	1.053
Lateral distribution	0.995	0.979
Longitudinal distribution	0.974	1.050
Deck flexure	1.023	1.019
Unintended comp. action	1.513	1.568

The contribution due to critical span adjustment applies only if the span instrumented in the field test differs from the

critical span determined for the analytical rating. It does not apply for the positive moment because the strain gauges were mounted at the same span (outer) as to where the maximum moment occurred. This contribution is less than 1.0 at the negative moment because the negative moment from the inner span loading is larger than the negative moment from the outer span loading. The contribution due to additional system stiffness accounts for other components in the bridge, such as curbs and railings. These components are not considered in the analysis and drive away the live load resisted by the girders. Therefore, the results are expected to be higher than 1.0. Although the values on the negative moment seemed to be accurate, the 27% increase observed on the positive moment may seem to be an overestimation. This inaccuracy may be caused by changes in the actual support condition due to accumulation of debris, which has a direct impact on the statical moment. If this value were true, the bridge owner could solely rely on this contribution to strengthen the bridge. The contribution due to lateral distribution accounts for the difference of the fraction of the moment carried by the critical girder relative to the total moment across the bridge in the actual and analytical load ratings. Minor differences between DF_A and DF_E are expected because the former is conservatively expressed as a function of the transverse girder spacing, whereas the actual lateral distribution of load also depends on the girder and edge stiffnesses [11]. The contribution due to longitudinal distribution accounts for the difference of moment distribution to the positive and negative moment positions in the actual and analytical load ratings. At the positive and negative moment positions, it was shown that the actual moment was almost as stiff as (3% and 5% difference, respectively) compared to the line-girder analysis. These differences show that more statical moment is going to the positive moment and less to the negative moment than predicted in the analysis. The contribution due to deck flexure represents the contribution besides the live load non-composite girder moment (M_{girder}) and interaction component of the live load moment ($N \times a$). This contribution is expected to be small (1% to 3%) because the curvature of the girder and deck deflection is the same, but the flexural stiffness of the former is much larger than the latter. The contribution due to unintended composite action accounts for the composite action developed between girder and deck for girders designed to be non-composite. In this study, it was observed that this contribution is dominant for both positive and negative moment positions. Although this effect is acceptable for a linear-elastic regime, it would become unreliable for loads beyond this limit. As a result, to determine a reliable ratio of load ratings, this contribution is divided out from the final value. Based on the load ratings calculated above, the ratio of the actual to the analytical load rating is equal to 1.90 at the positive moment and equal to 1.45 at the negative moment. The value is interpreted as the number of times that the actual load rating is relative to the analytical. If the contribution due to unintended composite action is removed, the ratio of the load ratings is then equal to 1.26 at the positive moment and equal to 0.93 at the negative moment. The reduction in the product for the negative moment reflects conservation of the statical moment (i.e., the load rating cannot simultaneously increase for both positive and negative moments). As a result, the actual reliable load rating is equal to 1.16 at the positive moment and 0.98 at the negative moment.

C. Comparison with Uncorrected Data

If the data were not corrected based on the fully composite action assumptions for Girders 1 through 4 at the positive moment, the ratio of load ratings would be equal to 1.90 at the positive moment and equal to 1.41 at the negative moment with the same respective controlling side-by-side vehicle loadings and critical girders. The values for each contribution are shown in Table 5 (the values of the variables for each contribution were not shown).

Table 5. Values of the contributions for the actual and analytical load rating comparison using Eq. (3) if no assumptions of composition action were made.

Contributions	Positive Moment	Negative Moment
Critical span adjustment	--	0.839
Additional stiffness	1.761	1.920
Lateral distribution	0.677	0.968
Longitudinal distribution	1.027	0.567
Deck flexure	1.023	1.019
Unintended comp. action	1.513	1.568

Although the values of the ratio of load ratings do not differ much from the values of the proposed procedure, it is possible to see that the contribution of additional stiffness, lateral distribution (positive), and longitudinal distribution (negative) are not realistic if no composite action corrections are made. For Girders 1 through 4, since the neutral axes of the strain profiles are below the girder centers of gravity in addition to a positive strain at the bottom of the bottom flange (Fig. 5), σ_{cg} is negative and so is $N \times a$. Even though a negative σ_{cg} contributes to the magnitude of M_{girder}, it is overweighted by the negative $N \times a$ which leads to a negative M_{total}. This reduces the values of $\sum STAT_E$ and DF_E and consequently affects the contributions due to additional stiffness, lateral and longitudinal distributions. As shown in Table 5, the contributions are unrealistic as they are significantly different from the analysis (it shows that the actual additional stiffness is almost twice the analytical, while the actual lateral and longitudinal distributions are almost cut in half). The contributions due to the deck flexure and unintended composite action were not affected because they only depend on the properties of the critical girder, which were not changed relative to the results of the proposed procedure.

V. CONCLUSION

In this paper, a procedure for a bridge field testing coupled with assumptions of composite action was described and

applied to a three-span five girder non-composite steel girder bridge located in Laramie, Wyoming. In the proposed procedure, the critical vehicle sequence for the bridge is determined, and the elastic response is measured for a series of vehicle tests by installing strain gauges at the critical positive and negative moment positions. To replace the data readings affected by the external effects, the position of the neutral axis corresponding to a fully composite action is assumed. After applying this correction, the actual load rating is discretized and compared with the analytical load rating so that different contributions to the loading capacity are quantified. For the bridge analyzed in this study, the results showed that the reliable load rating was equal to 1.26 and 0.93 at the positive and negative moment positions, respectively. Although the unintended composite action was the dominant contribution, it was removed because the bonding between girders and deck will likely be overcome for loads beyond the linear elastic regime. In addition, the results indicated that if assumptions of fully composite action for girders affected by external effects were not considered, the contributions due to additional stiffness, lateral and longitudinal distributions would have been unrealistic.

The study demonstrated that the proposed load rating procedure is a promising method to understand the behavior of highway bridges. In the proposed method, different contributions to the loading capacity are quantified and can be used in the decision-making process for maintenance, rehabilitation, and posting of highway bridges. The correction applied based on composite action is not only regarded as an alternative to replace data affected by external effects, but also can be adapted for field testing of highway bridges where mounting strain gauges on the web is not feasible (e.g., due to damages caused on the surface, lack of access, or desire to avoid impacting traffic flow). Additional analysis using a finite element model of the bridge is needed to accurately determine the degree of composite action.

REFERENCES

[1] D. B. Colleti, B. Chavel, and W. J. Gatti, “Challenges of skew in bridges with steel girders,” Transp. Res. Rec., vol. 2251, pp. 47-56, 2011.

[2] M. G. Barker, “Steel girder bridge field test procedures,” Constr. Build. Mater., vol. 13, pp. 229-239, 1999.

[3] R. Lu, Experimental load rating of skewed steel girder highway bridges, PhD dissertation, Dept. of Civil and Architectural Engineering, Univ. of Wyoming, 2020.

[4] M. G. Barker, “Quantifying field-test behavior for raitng steel girder bridges,” J. of Bridge Eng., vol. 6, pp. 254-261, 2001.

[5] M. Yarnold, T. Golecki, and J. Weidner, “Identification of composite action through truck load testing,” Front. Built Environ., vol. 4, pp. 74, 2018.

[6] BDI (Bridge Diagnostics Inc.), ST350 Operation Manual, Boulder, CO, 2012.

[7] AASHTO (American Association of State Highway and Transportation Officials), The Manual for Bridge Evaluation, 2nd ed., Washington, DC, 2011.

[8] C. R. Hendy, and F. Presta, “Transverse web stiffeners and shear moment interaction for steel plate girder bridges,” The Struct. Eng., vol. 86, pp. 017, 2008 [Proceedings of 7th International Conference on Steel Bridges, 4-6 June 2008, Guimarães, Portugal. ECCS, pp. 8, 2008].

[9] M. Sanayei, M., A. J. Reiff, B. R. Brenner, and G. R. Imbaro, “Load rating of a fully instrumented bridge: Comparison of LRFR approaches,” J. Perform. Constr. Facil., vol. 30, pp. 04015019, 2016.

[10] AASHTO (American Association of State Highway and Transportation Officials), Standard Specifications for Highway Bridges, 16th ed., Washington, DC, 1996.

[11] F. N. Catbas, H. B. Gokce, and M. Gul, “Practical approach for estimating distribution factor for load rating: Demonstration on reinforced concrete T-beam bridges,” J. Bridge Eng., vol. 14, pp. 652-661, 2012.